Peptide Self-Assembly

DOI: 10.1002/ange.201006897

Morphological Transformation between Nanofibers and Vesicles in a Controllable Bipyridine–Tripeptide Self-Assembly**

Damei Ke, Chuanlang Zhan, Alexander D. Q. Li, and Jiannian Yao**

One of the main challenges in self-assembly is to emulate biological systems and to design building blocks that have stimulus-responsive properties for programmed self-organization. In the past few decades, various building blocks arranged from β-sheet-forming peptides have been developed for synthetic well-defined architectures having potential applications in biomedicine, biomaterials, and optical and electronic materials.[1–3] Peptides offer distinct features including biocompatibility, highly ordered hydrogen bonds, ease of decoration with functional elements, and high stability of the β sheets.[4] In general, stimulus-responsive self-assemblies at the molecular level require a conformational change that leads to different secondary interactions and further molecular packing.[5] Considering the high stability of β sheets,[4] we aim to balance their conformational change and stability in stimulus-responsive self-assembly based on building blocks containing β-sheet-forming peptides (hereafter termed peptide building blocks). Accordingly, such a self-assembly is controlled at the β-sheet level[6] and morphological transformation is carried out on the basis of a "structural continuity of the stable β sheets". For example, transitions between plate nanoribbons and nanotubes rely on the capability of the twisting and unwinding of the plate nanoribbons.[6a] Transition between nanotubes and vesicles interrelates to the layered β sheets and the inner hollow nature.[6b] In addition, photoresponsive transition from quadruple helix to individual fibers is based on the fibril structures.[6c]

As a proof of principle, we designed an amphiphilic tripeptide–bipyridine conjugate **1** (Scheme 1). Two β-sheet-forming Lys-Phe-Ala peptides[7] are covalently linked at the 5,5′-positions of a hydrophilic bipyridine unit.[8] The sequence is designed as bipyridine–linker–Ala-Phe-Lys-Boc (Boc = *tert*-butoxycarbonyl) to produce possible U-shaped β-sheet-like structures in which the *N*-Cbz lysine (Cbz = benzyloxycarbonyl) side chains act as the hydrophobic U-shaped tails. U-shaped molecules have recently been reported to form vesicles.[9] The unprecedented cooperation between these functions leads to a controllable self-assembly forming vesicles and nanofibers. Surprisingly, external stimuli of temperature and ultrasound can further switch a reversible morphological transformation between vesicles and nanofibers.

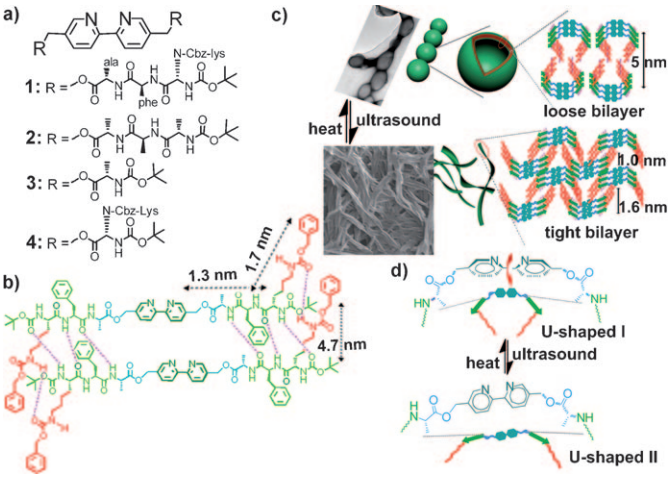

Scheme 1. a) Chemical structures of **1**–**4**. b) Hydrogen bonds and β-sheet-like structures formed from **1**. c, d) Proposed models for molecular packing and conformations of **1** inside vesicles (U-shaped I) and nanofibers (U-shaped II).

From the structural point of view, nanofibers and vesicles are distinctly different. Nanofibers are 1D nanostructures in which molecules tightly pack along the direction of 1D intermolecular interactions forming end-opened self-assemblies, whereas vesicles form a bilayer structure in which amphiphilic molecules have a hollow and spherical morphology, generally much larger than that of nanofibers. To the best of our knowledge, there are no reports regarding the morphological transition between these two structures based on regulating self-assembly by using peptide building blocks.

Compound **1** was successfully synthesized by coupling a tripeptide sequence of Boc-{(*N*-Cbz)-Lys}-Phe-Ala-COOH with 5,5′-dibromomethyl-2,2′-bipyridine in a yield of 70–80%. Analogues **2**–**4** were synthesized in a similar way. All conjugates were fully characterized by ^{1}H and ^{13}C NMR spectroscopy and mass spectrometry.

Although insoluble in water, **1** is soluble in tetrahydrofuran (THF). Addition of water to a THF solution of **1**, for example, up to a concentration of 2.0 mg mL^{-1} in 1:1 THF/water (v/v) led to the formation of vesicles (Figure 1a). The

[*] D. M. Ke, Dr. C. L. Zhan, Prof. Dr. J. N. Yao
Beijing National Laboratory for Molecular Sciences
Laboratory of Photochemistry, Institute of Chemistry, CAS
Beijing 100190 (P.R. China)
Fax: (+86) 10-8261-6517
E-mail: clzhan@iccas.ac.cn
jnyao@iccas.ac.cn
Prof. Dr. A. D. Q. Li
Department of Chemistry, Washington State University (USA)

[**] This work was financially supported by NSFC (Nos. 20973182, 20872145, and 20733006), the Chinese Academy of Sciences, 973 Projects (2006CB806200 and 2007CB936401), and NSF (CHE-0805547).

Supporting information for this article is available on the WWW under http://dx.doi.org/10.1002/anie.201006897.

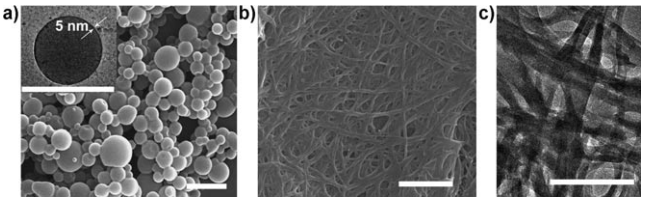

Figure 1. SEM and TEM images of a) vesicles and b, c) nanofibers obtained after ultrasound treatment of the transparent vesicle solution for 10 min ([**1**] = 2.0 mg mL^{-1}). Scale bars: 1 μm.

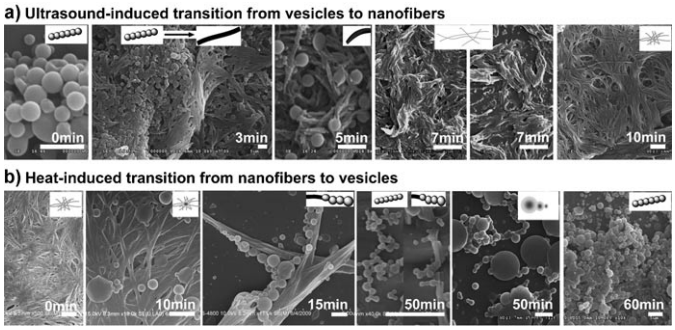

Figure 2. a) SEM observations of the conversion process from vesicles into nanofibers. A homogeneous solution of the vesicles was subjected to ultrasound for various periods. b) SEM observations of the conversion process from nanofibers into vesicles. The opaque gel was incubated at 60 °C in a water bath for various periods ([**1**] = 2.0 mg mL^{-1}). Scale bars: 1 μm.

hollow feature of the vesicles was clearly evidenced by transmission electron microscopy (TEM; inset of Figure 1 a). The wall thickness was estimated to be about 5 nm, consistent with a loose bilayer of the β-sheet-like structures in which **1** was proposed to adopt a conformation called U-shaped I (Scheme 1 c and d). In contrast, **2** and **3** without the lysine residue did not form vesicles under similar conditions. In fact, **2** formed rigid 1D nanoplates and **3** self-assembled into leaflike structures (Figures S1 and S2 in the Supporting Information). Moreover, the observation of vesicles from **4** pointed towards the vital role of the lysine residue in the formation of vesicles in our conjugates (Figure S3 in the Supporting Information).

Upon ultrasound treatment (0.40 W cm^{-2} and 40 kHz) of this vesicle solution for 10–30 min, an opaque gel formed. Scanning electron microscopy (SEM) and TEM images of the xerogels (Figure 1 b and c) revealed formation of micrometer-long fibril structures with sizes of 50–100 nm in width, which suggests an ultrasound-induced morphological transition from vesicles to nanofibers. No vesicles were observed, which indicates complete conversion of the vesicles to nanofibers. Interestingly, after the opaque gel was incubated at 60 °C in a water bath for about an hour, the nanofibers were fully transformed into vesicles and thus the gel was completely converted into the original transparent solution. This morphological transition was reversible and repeatable without any obvious fatigue effects, thus switching the macroscopic properties between transparent solution and opaque gel. It should be pointed out that compounds **2**–**4** exhibited no morphological changes upon heating and ultrasound treatment.

Ultrasound treatment led to collapse of the vesicles and subsequent formation of short nanoribbons, which further twisted under direction of chirality of the peptide segments and elongated into short nanofibers (Figure 2 a, 0–5 min). With the increase of treatment time, the short nanofibers became longer, and this finally led to the formation of nanofiber networks and consequential gelation (Figure 2 a, 7–10 min). Conversely, the reverse transition from nanofibers to vesicles most likely resulted from a process of heat-induced blooming of disklike microplates fused from the nanofiber networks (Figure 2 a, 10 min), accompanied by blooming of vesicles from the open end of nanofibers (Figure 2 a, 15–50 min). The mother microplates split into daughter vesicles with different sizes (Figure 2 a, 50 min).[1c] Because the nanofibers are insoluble, while the vesicles are soluble, the newly formed vesicles and microplates can disengage from the nanofiber networks and "dissolve" into the solution. This "dissolving" process may further facilitate the transition from nanofibers to vesicles.

What governs such a reversible transformation between nanofibers and vesicles? What are the differences in the conformations of the molecules inside the nanostructures, which may be sensitive to heat and ultrasound treatment and finally lead to the morphological change? To gain insight into the structural information inside the nanofibers and vesicles, a series of spectroscopic experiments was performed.

The X-ray diffraction (XRD) data (Figure 3 a) clearly reveal the formation of β-sheet-like structures. For the nanofibers, a very intense signal at $2\theta = 19.0°$ gives a d spacing of 4.7 Å, which is related to the spacing between peptide backbones.[10] In addition, several reflections were detected in the 2θ range of 5–12°, which originate from the ordered stacking periodicity of the β sheets (Scheme 1 c). The d value of 16.2 Å corresponds to the intersheet spacing between the

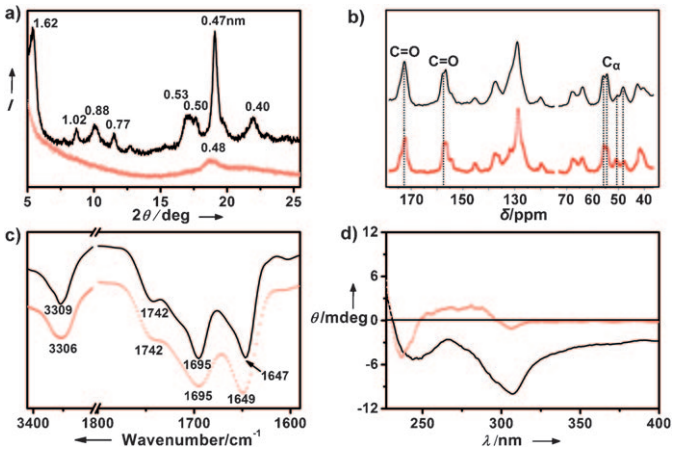

Figure 3. a) XRD patterns, b) solid-state CP-MAS ^{13}C NMR spectra, c) FTIR spectra, and d) CD spectra of the as-synthesized nanofibers (black lines) and vesicles (red lines; [**1**] = 2.0 mg mL^{-1}). The assigning of the CP-MAS ^{13}C NMR spectra is provided in detail in the Supporting Information (Figures S13 and S14).

lysine side chains, and values of 10.2, 8.8, and 7.7 Å are assigned to the intersheet periodicity between the phenylalanine side-chain packing at localized positions. Such an ordered stacking finally led to the formation of tight bilayers of the β-sheet-like structures in which **1** was considered to take a U-shaped II conformation. With regard to the vesicles, only one broad peak at $2\theta = 18.7°$ with a d spacing of 4.8 Å was detected, which had been assigned to the spacing between peptide backbones.[10]

The differences in diffraction peak numbers and relative intensities between these two sets of XRD data imply that the side chains of amino acid residues in fibril structures are in a more orderly and compact arrangement than those in the vesicles (Scheme 1c). The tight and loose bilayers are further supported by small-angle X-ray diffraction (SAXRD) data (Figure S5 in the Supporting Information): The peak with $d =$ 49.0 Å is consistent with the loose bilayers of the β-sheet-like structures in the vesicles and the peak at $2\theta = 3.1°$ is assigned to the orderly bilayered packing of the β-sheet-like structures in the nanofibers (Figure S6 in the Supporting Information).

Solid-state cross-polarization magic angle spinning (CP-MAS) ^{13}C NMR spectra confirm essentially the same patterns for the dipeptide segment of the Boc-{(*N*-Cbz)-Lys}-Phe sequence, which is bound by the backbone's hydrogen bonds inside both the nanofibers and vesicles (Figure 3b). The two amide-carbonyl peaks overlapped at approximately 172 ppm, which indicates that the dipeptide backbones adopt β-sheet-like rather than helixlike structures for which the resonances were expected at about 176 ppm.[11] The magnetic resonances of α carbon atoms of the lysine and phenylalanine residues occur respectively at 55.5 and 54.5 ppm for vesicles, and 55.8 and 54.4 ppm for nanofibers. Cbz and carbamate carbonyl peaks were observed at about 157.3 and 156.5 ppm for vesicles, and 157.7 and 156.7 ppm for nanofibers (Figures S13 and S14 in the Supporting Information), respectively.

These results suggest that the dipeptide segment adopts similar conformations inside both nanostructures. The nature of hydrogen bonding of the dipeptide segment is further confirmed by FTIR spectrometry (Figure 3c). The NH bands centered at 3309 cm^{-1} for nanofibers and 3306 cm^{-1} for vesicles are typical of NH functions involved in hydrogen bonding.[12] The amide I band at 1647 cm^{-1} for nanofibers but 1649 cm^{-1} for vesicles is also evidence for the β-sheet-like conformations.[13] The C=O stretching band at 1695 cm^{-1} is assigned to hydrogen-bonded carbamate and Cbz functions.[12] Thus, the overall set of data suggests 1) the formation of β-sheet-like structures in both nanostructures via intermolecular hydrogen-bonding networks of the Boc-{(*N*-Cbz)}-Lys-Phe segment (Scheme 1b) and 2) the stability of the β-sheet-like structures upon heat and ultrasound treatment.

Surprisingly, the CP-MAS ^{13}C NMR spectra show that the α carbon atoms of the alanine residues in both nanostructures are split into two bands at approximately 48.0 and 50.6 ppm, which arise from β-sheet and non-β-sheet forms, respectively.[11] Integrals indicated that only around 50% of the alanine residues in the vesicles and up to about 90% in the nanofibers were engaged in the β-sheet-like structures. This splitting reveals that up to 50% of the alanine residues inside the vesicles adopt different conformations, whereas in the nanofibers most of them select similar conformations. This conformational change resulting from ultrasound treatment is deeply related to the flexible nature of the linkers, as observed in ultrasound-induced gelation.[14] The flexibility of the linkers is further supported by FTIR spectra in which the C=O stretching band occurs at 1742 cm^{-1} (Figure 3c), which is attributed to unbound ester.[12,13a]

The ultrasound-induced conformational changes of the linkers may accompany different orientations of the bipyridine group in both nanostructures, as confirmed by circular dichroism (CD) experiments. Figure 3d shows that the CD signals of the nanofibers are totally different from those of the vesicles. Typical CD spectra of the nanofibers display two broad negative bands in the aromatic range. The broad negative band around 250 nm is attributed to a combination of the $n \rightarrow \pi^*$ transitions of bipyridine and $\pi \rightarrow \pi^*$ transitions of benzene groups.[15] The relatively strong CD signals around 295 (shoulder) and 306 nm originate from the characteristic bipyridine $\pi \rightarrow \pi^*$ transitions.[15a,b] In the vesicles, the bipyridine $\pi \rightarrow \pi^*$ transitions show a positive and negative Cotton effect at 278 and 307 nm, respectively, with a zero crossover at 291 nm. This reveals a quite different orientation of the bipyridine groups in the vesicles and nanofibers. Similarly, the benzene functions in the range of 250–285 nm show a positive Cotton effect in the vesicles, while in the nanofibers a negative Cotton effect arises at this band,[15c,d] further supporting the different packing of the peptide side chains in both nanostructures. The different packing of the side chains is consistent with the different positions of the aliphatic carbon atoms of the side chains occurring in the range of 45–10 ppm, for example, the β carbon atoms of the alanine (16.1 versus 18.2 ppm) and γ carbon atoms of the lysine residues (23.7 versus 25.9 ppm; Figures S13 and S14 in the Supporting Information).

Considering the large difference in the CD signals between both structures, variable-temperature CD spectroscopy was conducted to gain deeper insight into the conformational variety of the aromatics during the reversible morphological transition. Figure 4a and b show the recorded CD spectra during heating and cooling, respectively. Initial heating from 25 to 45 °C resulted in a slight increase in CD intensity, possibly as a result of the heat-induced dissolution of the nanofibers. When the temperature was above 55 °C, an obvious decrease of $[\theta]_{307}$ occurred. The sample was then kept at 60 °C for 40 min until no further changes in the CD spectra were observed. At this point, a spectral trajectory totally different from that of the nanofibers but similar to that of the vesicles appeared, which indicated full transition from nanofibers to vesicles. With the decrease of temperature from 60 to 25 °C, the $[\theta]_{307}$ value initially remained nearly constant and then increased when the temperature was below 35 °C, because of ordered packing of the molecules at lower temperature.

As inferred from the spectral data, the β-sheet-like structures formed from the terminal dipeptide segments are stable enough upon external stimulus. However, the flexible central linkers are free of hydrogen bonding, and thus possess high mobility and capability of conformational changes when subjected to heat and ultrasound. The intermolecular hydro-

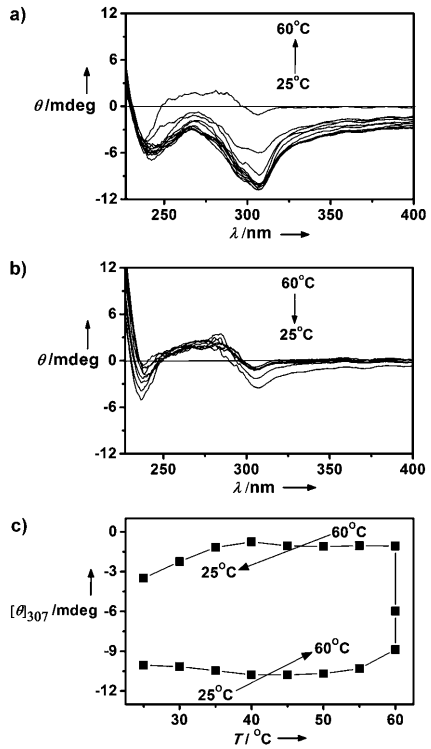

Figure 4. a, b) Temperature-dependent CD spectra of the morphological transition from nanofibers to vesicles in THF/water (1:1, v/v; [**1**] = 2.0 mg mL^{-1}). c) CD intensity at 307 nm as a function of temperature.

gen-bonding distance in the peptide segments is approximately 4.7 Å and the directionality of the β-sheet-like hydrogen-bonding network that coincides with packing of the flexible central linkers and hydrophilic bipyridine groups yields a much longer distance between the bipyridine units than the stable π···π stacking distance (ca. 3.4 Å).[16] Therefore, the bipyridine groups are mobile enough upon external triggering.

We propose that the reversible transition between the vesicles and nanofibers is related to a conformational variety of the flexible central linkers and the bipyridine groups adopting either loose or tight packing to accommodate structural changes in β-sheet-like bilayers when triggered by heat or ultrasound (Scheme 1c). Ultrasound treatment leads to collapse of the vesicles and formation of dense bilayer structures (Scheme 1c). This transformation is underpinned by the ultrasound-induced rotation of the bipyridine groups and a consequential conformational change of the flexible linkers (Scheme 1d). The directionality and the sticky nature of peptide hydrogen bonds are the driving forces in the dynamic self-assembly and elongation of the dense bilayers, which lead to the formation of nanofibers. As a result of the high stability of the bilayered β-sheet-like structures, the ultrasound-induced conformational changes of unbound flexible linkers and different orientations of the mobile bipyridine groups can be fully recovered when heating the nanofibers and this leads to the formation of vesicles.

In summary, we have reported a smooth and reversible transition between nanofibers and vesicles from a controllable self-assembly of an amphiphilic tripeptide–bipyridine conjugate. Such a morphological reversibility originates from a balance between the conformational change of the flexible central linkers and the stable β-sheet-like structures formed between the terminal peptide segments together with the mobile bipyridine units. Therefore, we have provided an elegant case to demonstrate how a small conformational change imparts morphological reversibility based on structural continuity of stable β sheets. This not only adds value in the understanding of stimulus-responsive self-assembly and morphological control from peptide building blocks, but also will be integrated into the design concept toward new artificial structures that mimic biological systems.

Received: November 3, 2010
Published online: February 15, 2011

Keywords: morphological transformation · nanofibers · peptides · self-assembly · vesicles

[1] a) F. Zhao, M. Ma, B. Xu, *Chem. Soc. Rev.* **2009**, *38*, 883–891; b) X. Yan, Q. He, K. Wang, L. Duan, Y. Cui, J. Li, *Angew. Chem.* **2007**, *119*, 2483–2486; *Angew. Chem. Int. Ed.* **2007**, *46*, 2431–2434; c) X. Yan, Y. Cui, Q. He, K. Wang, J. Li, W. Mu, B. Wang, Z. Ou-yang, *Chem. Eur. J.* **2008**, *14*, 5974–5980; d) B. Bulic, M. Pickhardt, B. Schmidt, E.-M. Mandelkow, H. Waldmann, E. Mandelkow, *Angew. Chem.* **2009**, *121*, 1772–1785; *Angew. Chem. Int. Ed.* **2009**, *48*, 1740–1752.

[2] a) K. J. Channon, G. L. Devlin, C. E. MacPhee, *J. Am. Chem. Soc.* **2009**, *131*, 12520–12521; b) K. J. Channon, G. L. Devlin, S. W. Magennis, C. E. Finlayson, A. K. Tickler, C. Silva, C. E. MacPhee, *J. Am. Chem. Soc.* **2008**, *130*, 5487–5491.

[3] a) S. R. Diegelmann, J. M. Gorham, J. D. Tovar, *J. Am. Chem. Soc.* **2008**, *130*, 13840–13841; b) L. Hsu, G. L. Cvetanovich, S. I. Stupp, *J. Am. Chem. Soc.* **2008**, *130*, 3892–3899; c) H. Shao, T. Nguyen, N. C. Romano, D. A. Modarelli, J. R. Parquette, *J. Am. Chem. Soc.* **2009**, *131*, 16374–16376; d) N. Ashkenasy, W. S. Horne, M. R. Ghadiri, *Small* **2006**, *2*, 99–102.

[4] a) S. Zhang, D. Marini, W. Hwang, S. Santoso, *Curr. Opin. Chem. Biol.* **2002**, *6*, 865–871; b) Y.-B. Lim, K.-S. Moon, M. Lee, *Chem. Soc. Rev.* **2009**, *38*, 925–934; c) I. Cherny, E. Gazit, *Angew. Chem.* **2008**, *120*, 4128–4136; *Angew. Chem. Int. Ed.* **2008**, *47*, 4062–4069; d) T.-B. Yu, J. Bai, Z. Guan, *Angew. Chem.* **2009**, *121*, 1117–1121; *Angew. Chem. Int. Ed.* **2009**, *48*, 1097–1101.

[5] a) S. Yagai, A. Kitamuraa, *Chem. Soc. Rev.* **2008**, *37*, 1520–1529; b) J. Wu, T. Yi, T. Shu, M. Yu, Z. Zhou, M. Xu, Y. Zhou, H. Zhang, J. Han, F. Li, C. Huang, *Angew. Chem.* **2008**, *120*, 1079–1083; *Angew. Chem. Int. Ed.* **2008**, *47*, 1063–1067; c) C. Wang, Q. Chen, F. Sun, D. Zhang, G. Zhang, Y. Huang, R. Zhao, D. Zhu, *J. Am. Chem. Soc.* **2010**, *132*, 3092–3096.

[6] a) H. Shao, J. R. Parquette, *Angew. Chem.* **2009**, *121*, 2563–2566; *Angew. Chem. Int. Ed.* **2009**, *48*, 2525–2528; b) P. P. Bose, A. K. Das, R. P. Hegde, N. Shamala, A. Banerjee, *Chem. Mater.* **2007**, *19*, 6150–6157; c) T. Muraoka, H. G. Cui, S. I. Stupp, *J. Am. Chem. Soc.* **2008**, *130*, 2946–2947.

[7] a) O. M. A. El-Agnaf, J. M. Sheridan, C. Sidera, G. Siligardi, R. Hussain, P. I. Haris, B. M. Austen, *Biochemistry* **2001**, *40*, 3449–3457; b) R. Vidal, B. Frangione, A. Rostagno, S. Mead, T. Révész, G. Plant, J. Ghiso, *Nature* **1999**, *399*, 776–781.

[8] a) D. E. Przybyla, J. Chmielewski, *J. Am. Chem. Soc.* **2008**, *130*, 12610–12611; b) D. E. Przybyla, J. Chmielewski, *J. Am. Chem.*

Soc. **2010**, *132*, 7866 – 7867; c) A. Richard, V. Marchi-Artzner, M.-N. Lalloz, M.-J. Brienne, F. Artzner, T. Gulik-Krzywicki, M.-A. Guedeau-Boudeville, J.-M. Lehn, *Proc. Natl. Acad. Sci. USA* **2004**, *101*, 15279 – 15284.

[9] a) C. Huang, L. Wen, H. Liu, Y. Li, X. Liu, M. Yuan, J. Zhai, L. Jiang, D. Zhu, *Adv. Mater.* **2009**, *21*, 1721 – 1725; b) Y. Li, X. Li, Y. Li, H. Liu, S. Wang, H. Gan, J. Li, N. Wang, X. He, D. Zhu, *Angew. Chem.* **2006**, *118*, 3721 – 3725; *Angew. Chem. Int. Ed.* **2006**, *45*, 3639 – 3643.

[10] a) O. Makin, L. Serpell, *Fiber Diffr. Rev.* **2004**, *12*, 29 – 35; b) P. Sikorski, E. Atkins, L. C. Serpell, *Structure* **2003**, *11*, 915 – 926; c) D. Ke, C. Zhan, X. Li, Y. Wang, A. D. Q. Li, J. Yao, *Tetrahedron* **2009**, *65*, 8269 – 8276.

[11] a) A. Shoji, T. Ozaki, H. Saito, R. Tabeta, I. Ando, *Macromolecules* **1984**, *17*, 1472 – 1479; b) H. R. Kricheldorf, D. Muller, *Macromolecules* **1983**, *16*, 615 – 623; c) H. Saito, R. Tabeta, A. Shoji, T. Ozaki, I. Ando, *Macromolecules* **1983**, *16*, 1050 – 1057; d) D. K. Lee, A. Ramamoorthy, *J. Phys. Chem. B* **1999**, *103*, 271 – 275.

[12] a) D. Bardelang, F. Camerel, J. C. Margeson, D. M. Leek, M. Schmutz, M. Badruz Zaman, K. Yu, D. V. Soldatov, R. Ziessel, C. I. Ratcliffe, J. A. Ripmeester, *J. Am. Chem. Soc.* **2008**, *130*, 3313 – 3315; b) E. Žagar, J. Grdadolnik, *J. Mol. Struct.* **2003**, *658*, 143 – 152.

[13] a) D. Ke, C. Zhan, X. Li, X. Wang, Y. Zeng, J. Yao, *J. Colloid Interface Sci.* **2009**, *337*, 54 – 60; b) T. Miyazawa, E. R. Blout, *J. Am. Chem. Soc.* **1961**, *83*, 712 – 719.

[14] a) Y. Wang, C. Zhan, H. Fu, X. Li, X. Sheng, Y. Zhao, D. Xiao, Y. Ma, J. Ma, J. Yao, *Langmuir* **2008**, *24*, 7635 – 7638; b) C. Baddeley, Z. Q. Yan, G. King, P. M. Woodward, J. D. Badjic, *J. Org. Chem.* **2007**, *72*, 7270 – 7278; c) T. Naota, H. Koori, *J. Am. Chem. Soc.* **2005**, *127*, 9324 – 9325; d) X. D. Yu, Q. Liu, J. Wu, M. Zhang, X. Cao, S. Zhang, Q. Wang, L. M. Chen, T. Yi, *Chem. Eur. J.* **2010**, *16*, 9099 – 9106; e) K. Isozaki, H. Takaya, T. Naota, *Angew. Chem.* **2007**, *119*, 2913 – 2915; *Angew. Chem. Int. Ed.* **2007**, *46*, 2855 – 2857.

[15] a) Y. Liu, X. Li, Y. Chen, X. Guan, *J. Phys. Chem. B* **2004**, *108*, 19541 – 19549; b) P. S. Braterman, B. C. Noble, R. D. Peacock, *J. Phys. Chem.* **1986**, *90*, 4913 – 4915; c) S. M. Kelly, T. J. Jess, N. C. Price, *Biochim. Biophys. Acta Proteins Proteomics* **2005**, *1751*, 119 – 139; d) C. Krittanai, W. C. Johnson, Jr., *Anal. Biochem.* **1997**, *253*, 57 – 64.

[16] a) H. W. Roesky, M. Andruh, *Coord. Chem. Rev.* **2003**, *236*, 91 – 119; b) X. Li, C. Zhan, Y. Wang, J. Yao, *Chem. Commun.* **2008**, 2444 – 2446.

